Supplement of Atmos. Chem. Phys., 24, 6495–6508, 2024
https://doi.org/10.5194/acp-24-6495-2024-supplement

Atmospheric Chemistry and Physics
Open Access

Supplement of

Daytime and nighttime aerosol soluble iron formation in clean and slightly polluted moist air in a coastal city in eastern China

Wenshuai Li et al.

Correspondence to: Daizhou Zhang (dzzhang@pu-kumamoto.ac.jp) and Yang Zhou (yangzhou@ouc.edu.cn)

S1. The influence of organic matters on aerosol pH

We utilized the same method of Guo et al. (2015) to calculated ALWCorg as the following equation:

$$ALWC_{org} = \frac{m_{org}\rho_w}{\rho_{org}} \frac{\kappa_{org}}{(\frac{100\%}{RH} - 1)}$$

where m_{org} is the OM concentration, which was estimated with 1.6 times OC (Turpin and Lim, 2001), ρ_w is water density (1.0×10^3 kg m^{-3}), and a typical organic density (ρ_{org}) of 1.4×10^3 kg m^{-3} was used. κ_{org} is the hygroscopicity parameter of organic aerosol compositions. We did not observe κ_{org} during the campaign, so we applied a typical range of 0.05−0.20 (Kuang et al., 2020). In Beijing, the typical κ_{org} of 0.06 was used in previous studies (Cheng et al., 2016). The higher the κ_{org} is, the larger the $ALWC_{org}$ would be. At last, we evaluated the range of $ALWC_{org}$ as 0.83−3.31 μg m^{-3}, which only accounted for 2.6−9.8% of the total ALWC. pH was about 2.49 without considering OM, and it was 2.52−2.57 when considering OM, indicating that the influence of OM in aerosol pH was very weak.

Reference:

Cheng, Y. F., Zheng, G. J., Wei, C., Mu, Q., Zheng, B., Wang, Z. B., Gao, M., Zhang, Q., He, K. B., Carmichael, G., Poschl, U., and Su, H.: Reactive nitrogen chemistry in aerosol water as a source of sulfate during haze events in China, Sci. Adv., 2, 11, 10.1126/sciadv.1601530, 2016.Guo, H., Xu, L., Bougiatioti, A., Cerully, K. M., Capps, S. L., Hite Jr, J. R., Carlton, A. G., Lee, S. H., Bergin, M. H., Ng, N. L., Nenes, A., and Weber, R. J.: Fine-particle water and pH in the southeastern United States, Atmos. Chem. Phys., 15, 5211-5228, 10.5194/acp-15-5211-2015, 2015.

Guo, H., Xu, L., Bougiatioti, A., Cerully, K. M., Capps, S. L., Hite Jr, J. R., Carlton, A. G., Lee, S. H., Bergin, M. H., Ng, N. L., Nenes, A., and Weber, R. J.: Fine-particle water and pH in the southeastern United States, Atmos. Chem. Phys., 15, 5211–5228, https://doi.org/10.5194/acp-15-5211-2015, 2015.

Kuang, Y., Xu, W., Tao, J., Ma, N., Zhao, C., and Shao, M.: A Review on Laboratory Studies and Field Measurements of Atmospheric Organic Aerosol Hygroscopicity and Its Parameterization Based on Oxidation Levels, Current Pollution Reports, 6, 410-424, 10.1007/s40726-020-00164-2, 2020.

Turpin, B. J. and Lim, H.-J.: Species Contributions to PM2.5 Mass Concentrations: Revisiting Common Assumptions for Estimating Organic Mass, Aerosol Science and Technology, 35, 602-610, 10.1080/02786820119445, 2001.

Table S1: Detection limits of the analysis instruments (unit: μg L^{-1} for WSIs and elements, and μg for OC and EC).

Species	DL_j	Species	DL_j
Na^+	20.0	V	0.0030
NH_4^+	20.0	Cr	0.0025
K^+	10.0	Mn	0.0055
Mg^{2+}	10.0	Fe	0.0139
Ca^{2+}	20.0	Ni	0.0287
F^-	10.0	Cu	0.0060
Cl^-	40.0	Zn	0.0770
NO_3^-	10.0	As	0.0151
SO_4^{2-}	10.0	Se	0.4062
$C_2O_4^{2-}$	10.0	Rb	0.0020
OC	0.20	Sr	0.0054
EC	0.20	Cd	0.0030
Al	0.0454	Ba	0.0022
Mg	0.0754	Pb	0.0026

Table S2: Classification results of aerosol samples.

Sample Types	Sample Number
Clean Periods Samples	19
Slightly-polluted Periods Samples	32
Heavily-polluted Periods Samples	6
Fog-impacted Samples	12
Dust-related Samples	70
Total	139

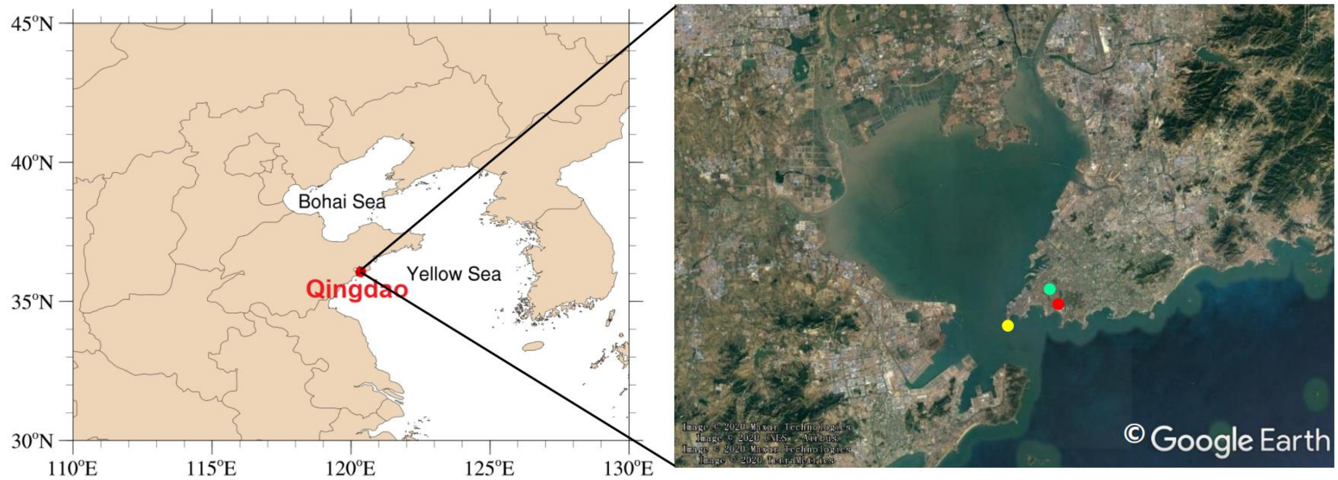

Figure S1: Location of the sampling site. In the right panel, the red dot shows the location of the sampling site. The green dot shows the location of Qingdao Meteorological Bureau. The yellow dot shows the location of the air quality monitoring station in Qingdao (the west sub-station of the Shinan District).

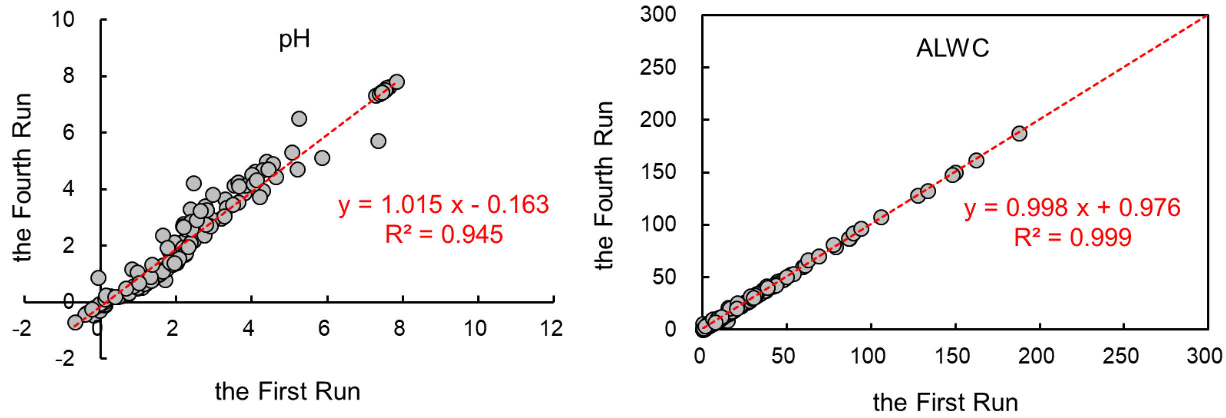

Figure S2: Relationships of aerosol pH and ALWC between the first run and the fourth run of ISORROPIA calculation.

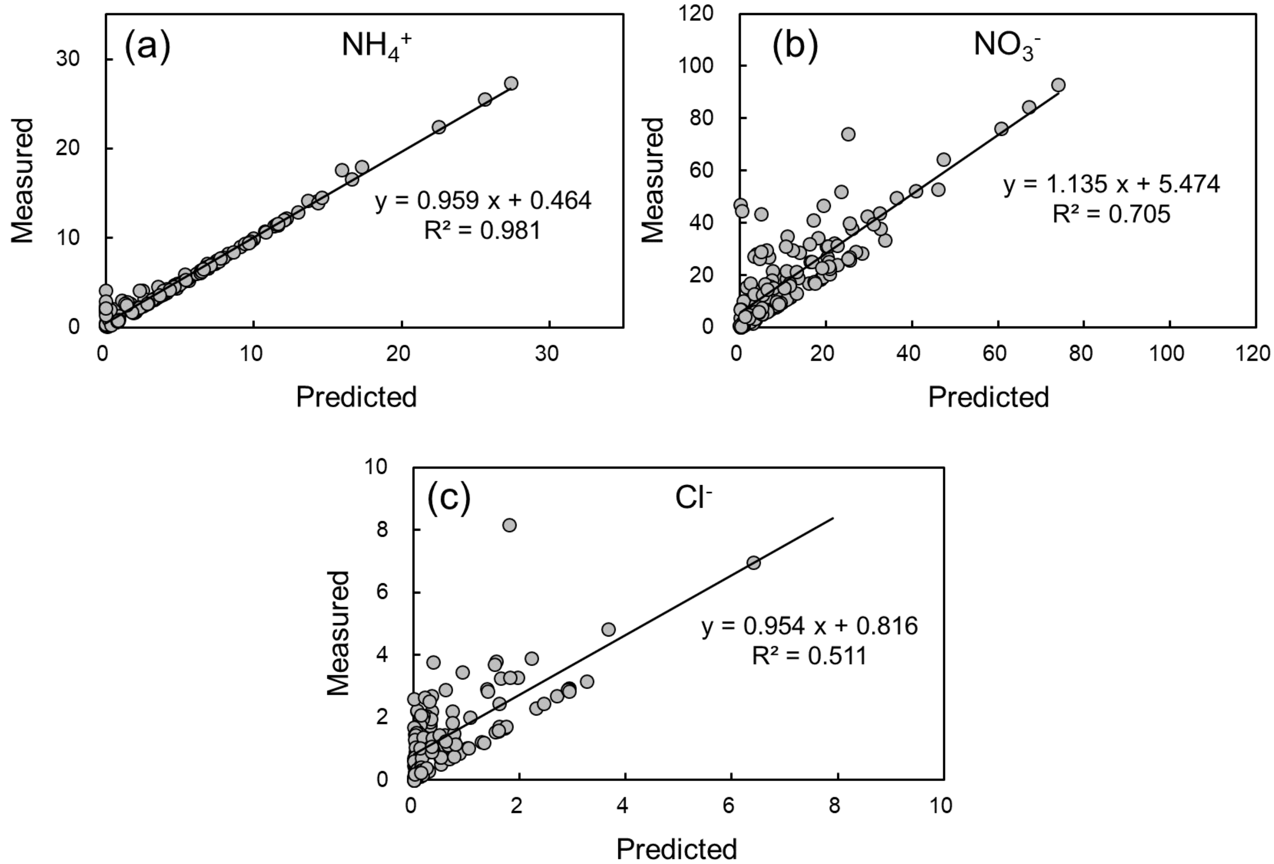

Figure S3: Intercomparisons of simulated and measured concentrations of NO_3^-, NH_4^+ and Cl^-.

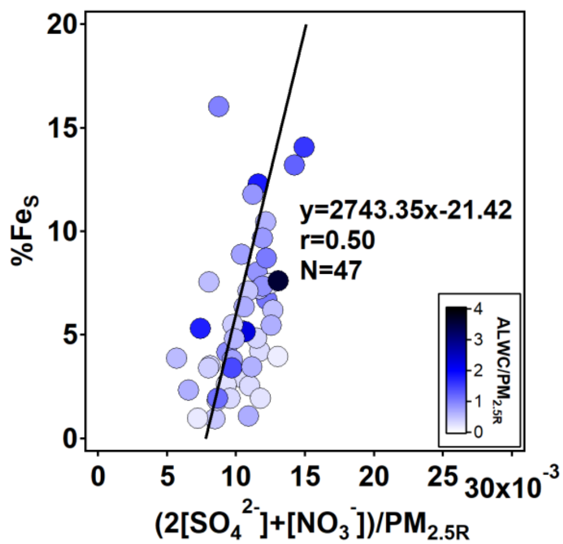

Figure S4: Same as Figure 3c in the manuscript but only for clean and SP periods.

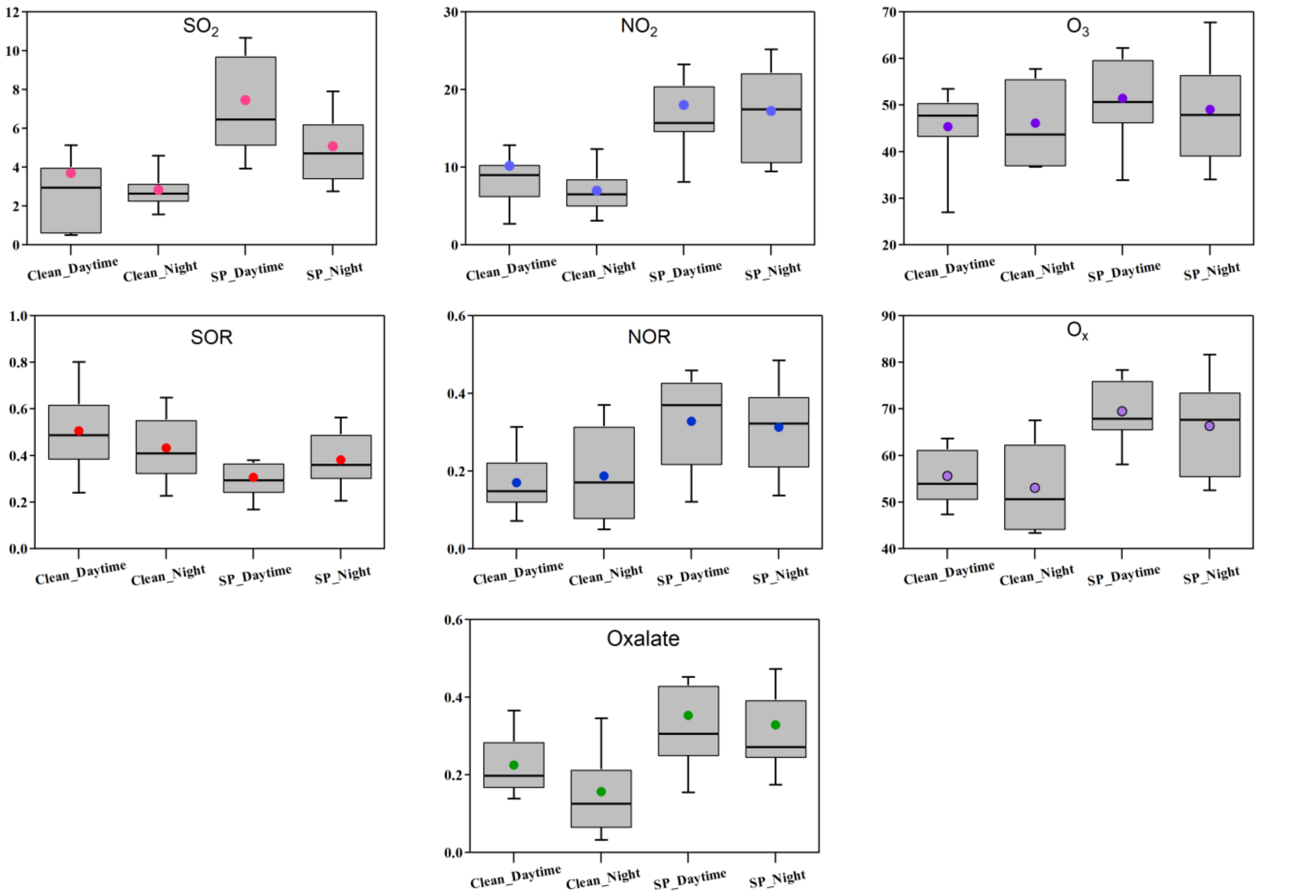

Figure S5: Box plots of several chemical parameters. Boxes represent the 25th, 50th and 75th percentiles. Error bars represent 10th and 90th percentiles. The dots within the boxes represent the arithmetic means.

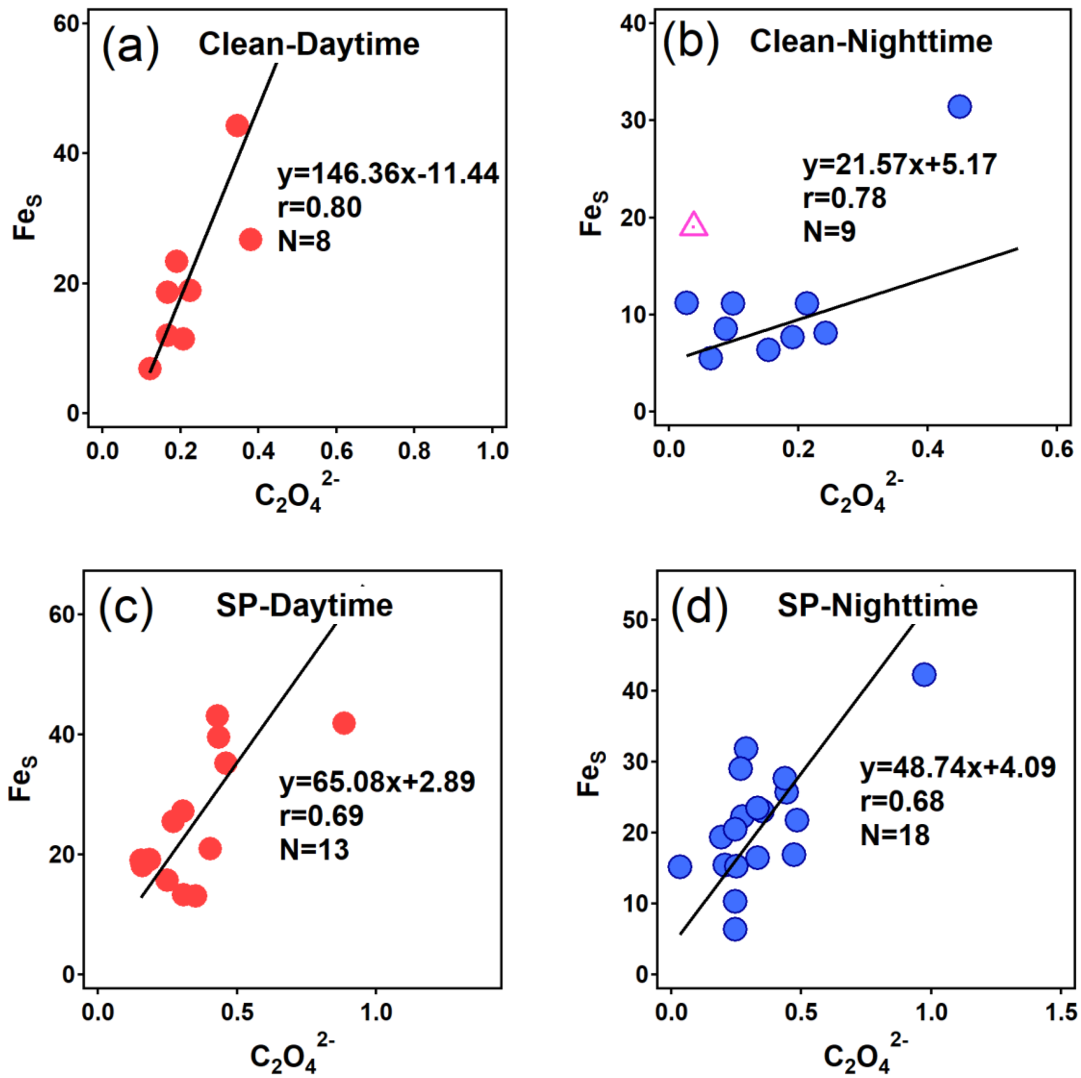

Figure S6: Relationships between soluble Fe (Fe_S, unit: ng m^{-3}) and oxalate (unit: μg m^{-3}). An extreme point (marked by a pink triangle, %Fe_S = 37.2%) in (b) was removed to obtain the more robust correlation coefficient.

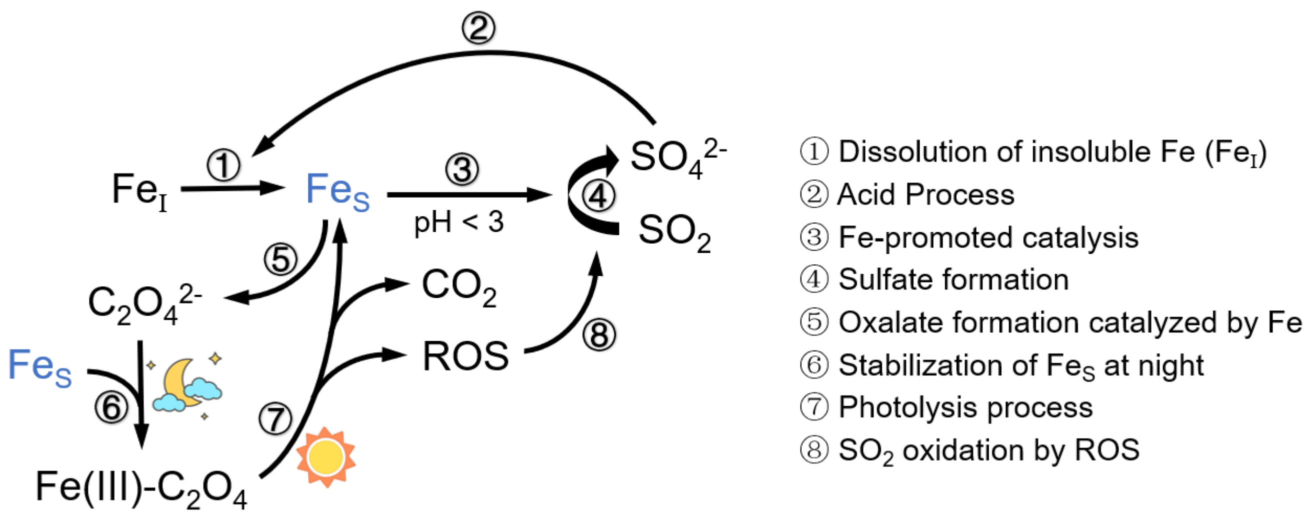

Figure S7: Conceptual diagram showing the Fe dissolution influenced by acid processes and oxalate.